



## Original Article

### Corresponding Author

P. Sarat Chandra

<https://orcid.org/0000-0002-3375-6803>

Department of Neurosurgery, All India  
Institute of Medical Sciences (AIIMS),  
Ansari Nagar, New Delhi 110029, India  
E-mail: saratpchandra3@gmail.com

Received: July 23, 2020

Revised: November 16, 2020

Accepted: November 17, 2020

See the commentary "From Anatomic to Genetic Understanding of Developmental Craniovertebral Junction Abnormalities" via <https://doi.org/10.14245/ns.2040548.274>.

See the commentary "Weak Ligaments and Sloping Joints: A New Hypothesis for Development of Congenital Atlantoaxial Dislocation and Basilar Invagination" via <https://doi.org/10.14245/ns.2040632.316>.



This is an Open Access article distributed under the terms of the Creative Commons Attribution Non-Commercial License (<https://creativecommons.org/licenses/by-nc/4.0/>) which permits unrestricted non-commercial use, distribution, and reproduction in any medium, provided the original work is properly cited.

Copyright © 2020 by the Korean Spinal Neurosurgery Society

## INTRODUCTION

Developmental bony craniovertebral junction (CVJ) anomalies frequently occur with neural abnormalities, indicating an embryologic relationship. They appear to be the result of maldevelopment of the cartilaginous neural cranium and adjacent

# Weak Ligaments and Sloping Joints: A New Hypothesis for Development of Congenital Atlantoaxial Dislocation and Basilar Invagination

Avnish K. Chauhan<sup>1</sup>, P. Sarat Chandra<sup>1</sup>, Nishant Goyal<sup>2</sup>, Madhumita R. Chowdhury<sup>3</sup>, Jyotirmoy Banerjee<sup>4</sup>, Manjari Tripathi<sup>5</sup>, Madhulika Kabra<sup>3</sup>

<sup>1</sup>Department of Neurosurgery, All India Institute of Medical Sciences, New Delhi, India

<sup>2</sup>Department of Neurosurgery, All India Institute of Medical Sciences, Rishikesh, India

<sup>3</sup>Genetics Center, All India Institute of Medical Sciences, New Delhi, India

<sup>4</sup>Department of Biophysics, All India Institute of Medical Sciences, New Delhi, India

<sup>5</sup>Department of Neurology, All India Institute of Medical Sciences, New Delhi, India

**Objective:** Developmental bony craniovertebral junction (CVJ) anomalies seem to have a genetic basis and also abnormal joint morphology causing atlantoaxial dislocation (AAD) and basilar invagination (BI).

**Methods:** DNA extracted polymerase chain reaction single-stranded conformation polymorphism (SSCP) performed for mutation screening of *FBNI* gene (n = 50 cases+ 50 age/sex-matched normal; total: 100). Samples with a deviated pattern of bands in SSCP were sequenced to detect the type of variation. Computed tomography (CT) scans of 100 patients (15–45 years old) compared with an equal number of age/sex-matched controls (21.9 ± 8.2 years). Joint parameters studied: sagittal joint inclination (SI), craniocervical tilt (CCT), coronal joint inclination (CI).

**Results:** Thirty-nine samples (78%) showed sequence variants. Exon 25, 26, 27, and 28 showed variable patterns of DNA bands in SSCP, which on sequencing gives various types of DNA sequence variations in intronic region of the *FBNI* gene in 14%, 14%, 6%, and 44% respectively. CT radiology: SI and CCT correlated with both BI and AAD (p < 0.01). The mean SI value in controls: 83.35° ± 8.65°, and in patients with BI and AAD: 129° ± 24.05°. Mean CCT in controls: 60.2° ± 9.2°, and in patients with BI and AAD: 86.0° ± 18.1°. Mean CI in controls: 110.3° ± 4.23°, and in cases: 125.15° ± 16.4°.

**Conclusion:** The study showed mutations in *FBNI* gene (reported in Marfan syndrome). There is also an alteration of joint morphology, correlating with AAD and BI severity. Hence, we propose a double-hit hypothesis: the presence of weak ligaments (due to *FBNI* gene alterations) and abnormal joint morphology may contribute to AAD and BI.

**Keywords:** Craniovertebral junction anomalies, Atlantoaxial dislocation, Basilar invagination, Fibrillin1 gene, Marfan syndrome, Joint morphology

vertebral skeleton during the early embryonic weeks.<sup>1,2</sup> The spectrum of congenital/developmental anomalies consists of atlantoaxial dislocation (AAD), and basilar invagination (BI), with occipitalization of C1 arch. Besides, there may be the presence of Os odontoideum, Chiari malformation (with or without syringomyelia), Klippel Feil anomaly, Clival segmentation

anomaly. Other uncommon anomalies include proatlas segmentation failure, condylar hypoplasia, bifid C1 arch, hemivertebrae. Besides, most of the patients we see have phenotypic markers (e.g., low set ears, hyper-extendibility, etc., see below). We frequently see developmental CVJ cases in the Indian subcontinent. We have used the term 'developmental' to indicate that even though the underlying pathology is congenital, the symptoms develop much later, usually the first or second decade of life.

The anomalies of the CVJ are associated with several connective tissue disorders,<sup>3-7</sup> and familial basis is also well documented<sup>8-13</sup> in the literature. As in most autosomal dominant disorders, we find a varied expression of clinical and morphological anomalies in congenital CVJ anomalies.<sup>14</sup> Earlier studies demonstrated an autosomal dominant trait for familial CVJ<sup>15,16</sup> (especially basilar impression).<sup>15,17</sup> Overall, many authors have viewed CVJ as a single autosomal dominant disorder expressed in a variable sequence as osseous malformations and Chiari malformation.<sup>14</sup>

More recently, we have demonstrated that deformed C1-2 joints may produce a mechanical disadvantage that itself may lead to a progressive deformity.<sup>18-26</sup> Probably, weight-bearing over a time coupled with age-related degenerative changes may precipitate BI and subsequently cause clinical features. Thus, many patients with congenital CVJ present with clinical symptoms present between first to the second decade of life and not during childhood.

Despite this evidence, there are very few studies till date, which have attempted to study developmental CVJ anomalies' genetic basis.<sup>25,27</sup> We found that most studies were based on the Caucasian population on genome-wide association (GWAS)<sup>28</sup> and tagged SNP's.<sup>29</sup> Boyles et al.<sup>28</sup> in a GWAS, screened genome-wide linkages with 71 affected individuals and analyzed over 10,000 single-nucleotide polymorphisms (SNP) across the genome and found linkage to regions on chromosome 9 and chromosome 15, at loci 15q21.1-q22.3 and 9q22.31. They found the fibrillin1 gene (*FBN1*) on chromosome 15, as the most biologically plausible gene for Chiari malformation I (CMI). *FBN1* is known to encode for the gene for fibrillin. Three different genes *FBN1*, *FBN2*, and *FBN3* encodes fibrillins in humans. Fibrillins are large (~350,000 MW) structural macromolecules that not only contribute to the integrity and function of all connective tissues but also target and sequester members of the transforming growth factor- $\beta$  superfamily of growth factors and contribute to organ formation and repair.<sup>30</sup> Thus mutations in fibrillins can contribute effectively to tissue growth

and homeostasis. Each fibrillin molecule contains 47 epidermal growth factor (EGF)-like domains, 43 are predicted to bind to calcium (cbEGF), 7 8-cysteine containing domains (8-cys), 2 "hybrid" domains that share features of both the 8-cysteine domain and the EGF-like domain, a proline-rich domain, and amino- and carboxyl- terminal domains.<sup>30</sup> Genetic studies revealed mutations in the fibrillin molecules as an essential determinant in clinical phenotypes of Marfan syndrome (MFS). Till now, 1,847 different mutations in 3,044 DNA samples have been reported in the *FBN1* mutation database (<http://www.umd.be/FBN1/>- last updated 8/28/2014). Mutations related to atypically severe phenotypes were found to be clustered in exons 24-32 in MFS.<sup>31</sup> This region is composed of a central longest stretch of 12 cbEGF repeats, which is believed to form a rigid rod-like structure with a crucial role in microfibril assembly. Also, genotype-phenotype correlations of mutations in *FBN1* are associated with specific clinical features of MFS. The most consistent correlation was found in the middle region of the gene (exons 24-32) with all cases of "neonatal" MFS and its other severe forms.<sup>32-34</sup> Despite these studies, the exact phenotype for any given *FBN1* mutation is not predicted so far.

Considering that fibrillin is an important component of microfibrils, we hypothesized that mutations in *FBN1* might precipitate BI and AAD by causing loss of structural integrity of ligaments. Since the *FBN1* gene is quite large, we planned first to study exons 24-28, which are also hotspots for mutations in MFS. Then we screened the rest of the 60 exons in 20 patients. To best of our knowledge, this is the first of its kind of study involving this category of patients. We also correlated the study with joint morphology study in 100 patients with developmental AAD and BI.

## MATERIAL AND METHODS

### 1. Ethics Statement

The Institute Ethics Committee approved the study. A detailed written consent was taken from both the patients and control samples explaining to them the study's details and possible outcome.

The main inclusion criteria for the study was the presence of a nonsyndromic structural CVJ anomaly. All patients included in the study had BI with AAD. Besides, the various other radiological features included one or more of these features: occipitalization of C1 arch, clival segmentation anomalies, Chiari malformation, hydrocephalus, and/or os odontoideum. We have not included patients with specific known genetic syndromes

in this study e.g., Down syndrome. Similarly, we excluded all patients with traumatic or inflammatory etiologies.

All patients underwent a complete clinical work up, and the phenotypic features carefully noted (Figs. 1, 2). Imaging included magnetic resonance imaging (MRI) (with contrast) of the CVJ with whole spine screening and a computed tomography (CT) scan. The CT scan consisted of thin-slice bone windows with sagittal and coronal reconstruction.

The control included healthy subjects, who had attended the outpatient department with trivial noncongenital problems (e.g., degenerative neck or back problem) and consented to give their blood samples. All the subjects included in the study were from the same ethnic Indian population.

**2. Collection of Samples for Genetic Studies**

Venous blood samples measuring 5 mL were obtained in eth-

ylenediaminetetraacetic acid (EDTA) tubes. Control samples (50 healthy subjects, 100 reference alleles) were taken from the general healthy population presenting to the outpatient department either with trivial noncongenital problems (e.g., degenerative neck or back pain) or were healthy attendants of the patients who consented to provide their blood.

**3. DNA Isolation and Quantification**

Genomic DNA was extracted using conventional phenol-chloroform method.<sup>35</sup> Amplification<sup>36</sup> of 65 exons of *FBNI* gene was carried out in a 25-µL reaction volume using 50 ng of genomic DNA as a template and 10 pmol of each primer (Table 1),<sup>37</sup> buffer with a final Mg2+ concentration of 3.7mM, 0.75mM of each dNTP and 0.5U Taq polymerase. The amplifications were carried out using the following cyclic conditions: initial denaturation at 95°C for 10 minutes, followed by 30 cycles at



**Fig. 1.** Clinical features (phenotypic) of the patients with developmental bony craniovertebral junction anomalies. (A) Mongoloid slant, hypertelorism, (B) short neck, low set ears, (C) short neck, (D, E) torticollis, (F) short neck and low set ears, (G) torticollis, short neck, (H) hypertelorism, (I) low set ears, (J) torticollis, (K) short neck, (L) low set ears, (M) torticollis, (N) low set ears, (O) torticollis, and (P) hypertelorism.

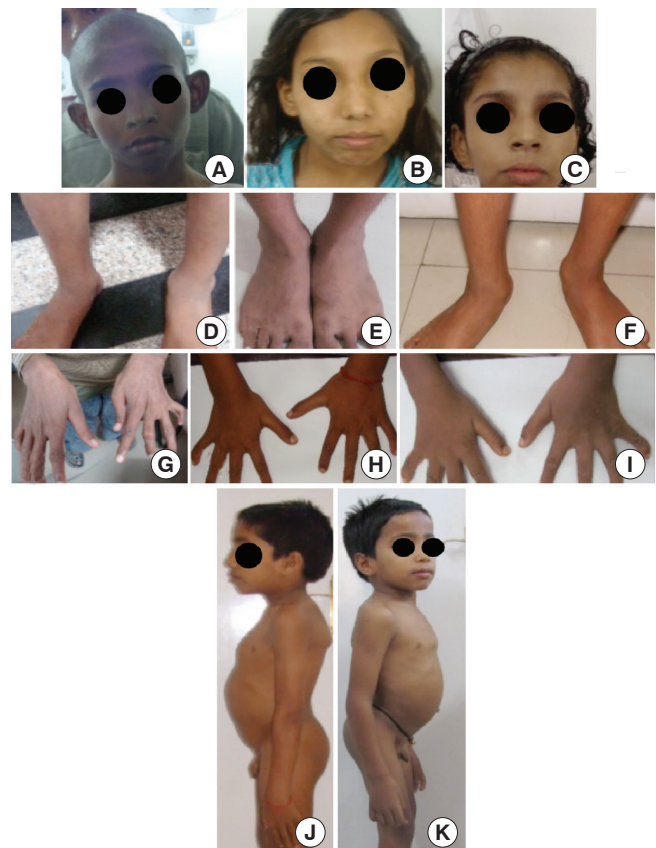


**Fig. 2.** Clinical features (phenotypic) of the patients with developmental bony craniovertebral junction anomalies. (A) Hypertelorism, (B) hypertelorism and mongoloid slant, (C) hypertelorism (D-F) increased first interdigital space, (G) arachnodactyly, (H, I) clinodactyly, and (J, K) whole-body images of the patients.

**Table 1.** Values of various indices (both conventional and those measured in this study, n = 50 each)

Parameter	Cases	Controls	p-value
Atlanto-dens interval	5.4 ± 3.2	1.0 ± 0.2	< 0.01*
Wackenheim clival canal line	-5.3 ± 4.4	2.7 ± 1.8	< 0.01*
Chamberlain line	-8.1 ± 4.2	2.9 ± 3.1	< 0.01*
Mc rae line	-2.3 ± 3.4	5.4 ± 1.2	< 0.01*
Modified ranawat line	18.8 ± 4.3	26.1 ± 2.5	< 0.01*
Craniocervical tilt (°)	86.0 ± 18.1	60.2 ± 9.2	< 0.01*
Coronal inclination (°, average for both)	125.15 ± 16.4	110.3 ± 4.23	0.12
Sagittal inclination (°, average for both)	129 ± 24.05	83.35 ± 8.65	< 0.01*

Values are presented as mean ± standard deviation.

Length in mm, area in mm<sup>2</sup>, negative value indicates level above foramen magnum.

\*p < 0.05, statistically significant difference.

95°C for 25 seconds, for annealing a range of temperature from 55°C–60°C for 25 seconds were used, followed by 72°C for 25 seconds, and a final extension at 72°C was given for 10 minutes.

### 1) Mutation screening

The amplified products were screened using single-stranded conformation polymorphism (SSCP)–heteroduplex<sup>37</sup> analysis. Polymerase chain reaction products were denatured in formamide dye (0.01M EDTA, 98% formamide, trace xylene cyanol, and bromophenol blue) and run on 8% polyacrylamide gels (acrylamide 49:1) for 16 hours at 250 V and silver stained. The samples which migrate differently in SSCP–heteroduplex analysis were sequenced using a fluorescent cycle-sequencing kit. Sequencing conditions consisted of initial denaturation for 1 minute at 96°C; 30 cycles of 96°C for 30 seconds, 15 seconds at 50°C, and 60°C for 4 minutes. Bidirectional sequencing was performed for all the samples exhibiting shifts using ABI 3130 genetic analyzer (Applied Biosystems, Alameda, CA, USA). The sequencing results were compared with the original data using NCBI BLAST (Gen Bank Accession No. AC022467 and AC 084757) and typical *FBN1* reference sequence (ENST00000316623). All sequence variations were analyzed in both control, and patient samples and the presence of the mutations were reported in terms of percentage.

### 2) Radiological measurement of joint morphology

The study population comprised of 100 patients with ‘non-syndromic, developmental bony CVJ anomalies with BI and AAD’ (see below for definition) with an occipitalized C1 arch in the age range of 15 to 45 years old. Patients of < 15 years of age were excluded due to incomplete physiological bony fusion, and patients of > 45 years of age were excluded because of ex-

pected degenerative changes.<sup>38</sup> Besides, the following patients were also excluded: (1) traumatic AADs, (2) polytrauma involving other areas of the cervical spine, (3) rheumatoid arthritis, (4) inflammatory pathologies, such as tuberculosis, (5) patients where imaging did not show the clivus or hard palate, and (6) known genetic syndromes, such as Down or Marfan.

#### (1) Nonsyndromic, developmental CVJ anomalies

These anomalies included various bony irregularities that suggest a congenital origin, including one or more of the following: occipitalization of the C1 arch with or without fusion at other levels, os odontoideum, clival segmentation anomalies, and Chiari malformation. The features of AAD and BI were observed in all patients and formed the primary inclusion criteria for patients. The patients had one or more of the following phenotypic features: low hairline, short neck, low set ears, clinodactyly, increased first interdigital space of the foot, hyperelastic joints, and arachnodactyly. None of the patients had any known genetic syndrome anomalies.

#### (2) Controls

The control group included an equal number of age and sex-matched subjects who had undergone a CT scan of the cervical spine and CVJ as a part of the screening procedure following minor injuries. We included only those patients without any evidence of trauma to the cervical spine and CVJ.

#### (3) Radiological studies

All craniometric measurements were performed using CT rather than x-rays and MRI's because of the better identification of the bony landmarks on the CT scan.

Thin-slice CT scans (0.63 or 0.7 mm) with reconstructed

views were used. All scans were obtained on a 64-MDCT scanner (Aquilion 64, Toshiba Medical Systems, Otawara, Japan) using a rotation time of 500 msec, a tube voltage of 120 kV, and a tube current 40–369 mA. The acquired images were reconstructed into 0.63-mm-thick CT images in 3 orthogonal planes on a dedicated workstation using 3-dimensional software (Vitre 2, Vital Images, Minnetonka, MN, USA). The midsagittal

plane was reconstructed by realigning the positioning crosshairs on the axial images. Images were analyzed on a preset bone window setting of a 2700 HU width and a length of 350 HU.

#### (4) Measurements

The radiological parameters included atlantodental interval (ADI),<sup>39</sup> and Wackenheim clival canal line, Chamberlain line,

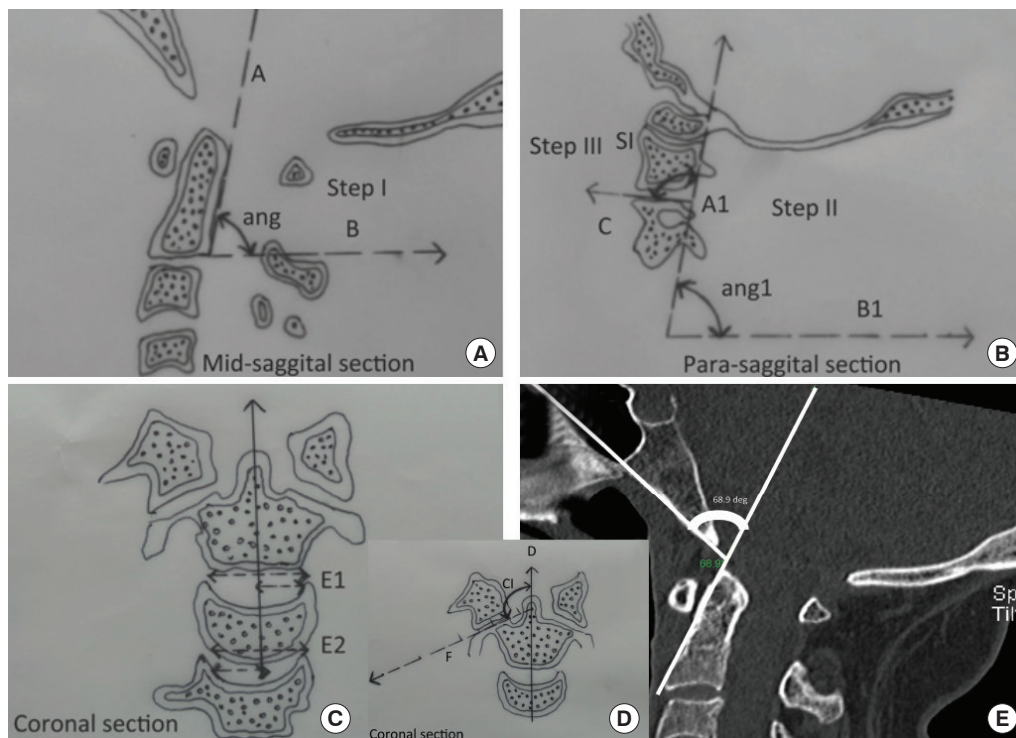


**Fig. 3.** This figure shows the method of calculating the sagittal joint inclination. This is the angle between the long axis of the odontoid process and the surface of the C1–2 joint. However, because the odontoid process is in the midline and the C1–2 joint is at the level of the parasagittal section, the following method to measure this angle was used. (A, B) Step I: In the midsagittal section, a line is drawn along the posterior border of the odontoid process (line A). Next, a line is drawn parallel to the border of the image (line B), which now subtends an angle “ang” (panel A). (B) Step II: This step is performed in the parasagittal section, where the joints are visible. In this step, a line is first drawn parallel to the border of the image (line B1, panel B). Next, the same angle value is constructed as in “ang” (here “ang1”, panel B) with another line A1 that now passes along a point on the posterior border of the C2 joint surface. (B) Step III: This step is also performed in the parasagittal section. In this step, a line is drawn that passes parallel to the C2 facet joint (line C, panel B). The angle now subtended between the lines A1 and C are called as the sagittal joint inclination (SI). The horizontal line B that is drawn in the midsagittal section (A, B) should be parallel to the border of the film. It may be drawn at any distance from the lower border of the image. Because the entire computed tomography is performed on the patient at the same time point in time, this line will have the same referential value in the midsagittal and parasagittal sections. Hence, this line is useful to measure the angle between the long axis of the odontoid process and the C1–2 joint, which is the sagittal SI. (C) This figure shows the method to measure the coronal SI, which is the angle between the long axis of the odontoid process and the C1–2 joints in the coronal plane. In the midcoronal section, where the C2/C1 joint is visible, the midpoints of 2 lines joining the uncinat processes of C2 and C3, respectively, are first marked (here as E1 and E2, panel C). A line joining these 2 points (called line D, panel D, inset) is drawn extending upwards. Another line (line F) is drawn parallel to the upper border of the C2 joint, which joins with line D (panel D). The angle subtended between the lines D and F is called the coronal SI. (E) This figure shows the method to measure the craniocervical tilt. This angle is measured between the long axis of the odontoid process and the clivus. A line is drawn first along the anterior border of the odontoid process and extended upwards. Next, a line is drawn along the anterior border of the clivus. The angle subtended between these 2 lines is called the craniocervical tilt (see text for more details).

McRae line, and modified Ranawat's line were used to measure BI.<sup>25,40-44</sup> All these techniques have been previously described.<sup>25</sup>

The following joint dimensions were measured bilaterally. These have been described earlier.<sup>20,22-24,26</sup> These include sagittal and coronal joint inclinations, and craniocervical tilt.<sup>20,22-24,26</sup> The details of these measurements have been shown in Fig. 3.

We performed the data analysis using IBM SPSS Statistics ver. 20.0 (IBM Co., Armonk, NY, USA). We used the independent t-test for assessing the continuous numerical parameters comparing patients and controls. For the correlation between 2 continuous numerical values, we used the Pearson correlation test.

#### (5) Other investigations

All patients underwent a complete systemic examination. x-ray chest, electrocardiogram, and a cardiological examination was performed to look for any cardiac anomalies. Dual-energy x-ray absorptiometry scans and osteoporosis work was performed when required. Vitamin D3 was performed in all patients. In patients with low Vitamin D3, supplementation was provided before admission. Ultrasound abdomen was performed to look for any anomalies in abdomen and bladder.

## RESULTS

### 1. Clinical Profile

We included 50 cases and compared them with equal number of age and sex-matched controls. The age of the patients ranged from 8–61 years (mean age, 40.6 ± 12.4 years). The clinical features included neck pain (48 cases, 96%), numbness of the limbs (44 cases, 88%), and unsteady gait (43 cases, 86%) (Table 2). The phenotypic features included low set ears (41 cases, 82%), followed by clinodactyly (30 cases, 60%) and increased the first interdigital space of the foot (26 cases, 52%) (Figs. 1, 2). The commonest radiological finding was BI (34

cases, 68%), followed by AAD (31 cases, 62%) and clival segmentation (29 cases, 58%). Statistical comparison of genetic differences with the control group could not be done as all the mutations were observed in 78% of the disease cohort and 0% in the control group. None of the patients in our cohort had any systemic cardiac and skeletal anomalies.

### 2. Genetic Profile (Figs. 4-7)

Thirty-nine samples (78%) showed sequence variants. Exon 25, 26, 27, and 28 showed variable patterns of DNA bands in SSCP, which on sequencing gives various types of DNA sequence variations in intronic region of the *FBNI* gene in 14%, 14%, 6%, and 44% respectively. We observed a total of 7 shifts in 7 patients (14%) in exons 25 and 26 (on sequencing identified as 6 base pair deletion as delTCTTTA). In exon 27, 3 similar shifts were observed (n=3, 6%). The sequencing here showed a substitution (c.3575C>G), leading to a change in amino acid sequence proline to alanine (P.P1148A). In contrast, exon 28 revealed several shifts in SSCP in 44% of the cohort (n=22). The sequencing here showed 2 different deletions and one substitution in the intronic region. Other changes include detection of delGTTAT (5-base pairs: del GTTAT, 3589+67\_3589+71) in 14% (n=7); detection of delTTTTTA (also a 5-base pairs, present in combination with a substitution 3792-5 G/A) in 14% (n=7). Glutamine/arginine (G/A) was found in with delTTTTTA in exon 28. It is also remarkable that the exon 27 (P1148A) change is entirely concordant with the substitution G/A. DNA shifts were not seen in the SSCP gels in the rest of the exons. No shifts were obtained in the control population on SSCP gels in exon 24, 25, 26, and 27, whereas in exon 28, shifts were obtained and identified as delGTTAT. A statistical comparison of genetic differences with the control group could not be done as all the mutations were observed in 78% of the disease cohort and 0% in the control group.

#### (1) Radiological examination

The study group was comprised of 100 patients (64 males, 26 females) and compared with an equal number of age- and sex-matched controls (total 140 subjects). The mean age of the patients and controls was 21.9 ± 8.2 years.

The values for all the various parameters (patients and controls) are as shown in Table 1. Using receiver operating characteristic curves, the Chamberlain line's distance, with zero as the cutoff, had the best sensitivity and specificity.

The most frequent anomaly was BI (n=35, 72%) followed by AAD (n=33, 66%) and clival segmentation defects (n=18,

**Table 2.** Correlation between the atlantoaxial interval and various joint morphometric parameters

Parameter	Strength of correlation	p-value
Craniocervical tilt	44.5%	< 0.01**
Right coronal inclination	4.1%	0.78
Left coronal inclination	-26%	0.06
Right sagittal inclination	-60.6%	< 0.01**
Left sagittal inclination	-53.7%	< 0.01**

\*\*p < 0.01, statistically very significant difference.

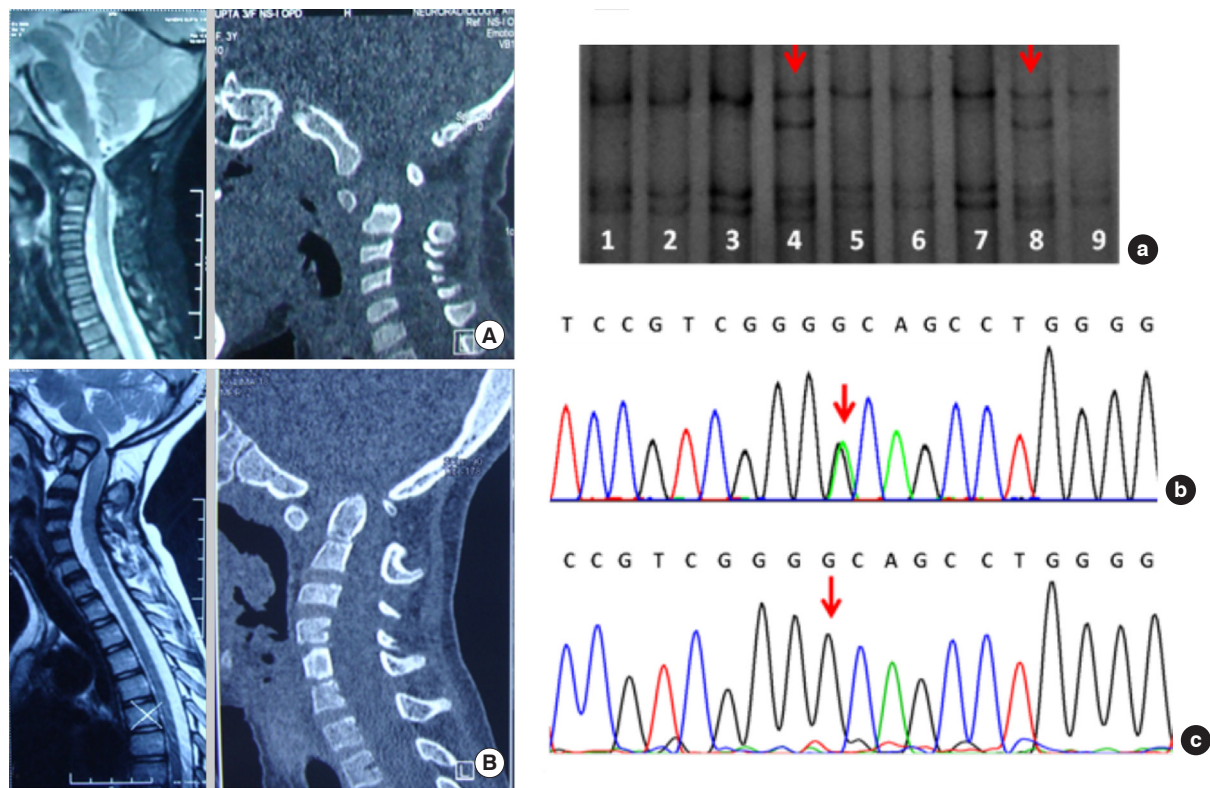


**Fig. 4.** Radiological profile of patients with change c.2956G > A/p.Ala986Thr in exon 24 in the *FBNI* gene. (A) Magnetic resonance imaging (MRI) and computed tomography (CT) scan of patient P1 showing atlantoaxial dislocation. (B) MRI and CT scan showing basilar invagination and atlantoaxial dislocation. (Right panel) single-stranded conformation polymorphism (SSCP) and sequencing analysis of variant p.A986T (a) SSCP gel picture showing the DNA band shifts in lane 4 and 8 (indicated by arrow). (b) Chromatogram developed by DNA sequencing showing the heterozygous change G > A at position. (c) Chromatogram of the same region of the normal control sample.

36%). This was followed by CMI (n=9, 18%), occipitalized C1 (n=8, 16%), syringomyelia (n=8, 16%), os odontoideum (n=4, 8%), platybasia (n=3, 6%), Klippel Fiel anomaly (n=2, 4%) and atlas assimilation (n=2, 4%)

The mean ADI in patients (Table 1) with BI and AAD was  $5.5 \pm 3.2$  mm (the ADI in controls was  $1.0 \pm 0.3$  mm). The mean distance of the dens in patients with BI and AAD above Wackenheim's clival canal line was  $5.5 \pm 4.4$  mm (in controls, the dens was  $2.6 \pm 1.8$  mm below this line), the mean distance above Chamberlain's line in patients was  $8.3 \pm 4.2$  mm (in controls, the dens was  $2.9 \pm 3.3$  mm below this line). The mean distance above McRae's line in patients was  $2.5 \pm 3.4$  mm (in controls, the dens was  $5.2 \pm 1.2$  mm below this line). The mean values of the modified Ranawat's line were  $18.8 \pm 4.4$  mm and  $26.1 \pm 2.5$  mm for patients and controls. The differences between patients and controls for all values were significant ( $p < 0.01$ ). Table 2 shows the strength of the atlanto dental interval and various joint indices.

The comparison of the severity of AAD with the various joint

indices revealed that there was a significant correlation with the sagittal inclination (SI) and the craniocervical tilt (both  $p < 0.01$ ) (Table 1). When the severity of BI (Chamberlain's line) was compared (Tables 1, 2) with various joint indices, it strongly correlated with the SI and craniocervical tilt (both  $p < 0.01$ ). Besides, the joint reciprocity ( $p = 0.04$  for left side, 0.01 for right side) correlated with the BI. Thus, the joints, which had a higher coronal joint inclination and were nonreciprocal joints, were more prone to develop BI. The correlation with coronal joint inclination ( $p = 0.16$  for left side, 0.2 for right side), joint surface area and overlap index failed to reach significance with both AAD and BI.

The mean SI for controls was  $83.35^\circ \pm 8.65^\circ$ , and in patients with BI and AAD, it was  $129^\circ \pm 24.05^\circ$  ( $p < 0.01$  for both BI and AAD). The mean craniocervical tilt for controls was  $60.2^\circ \pm 9.2^\circ$ , and in patients with BI and AAD, it was  $86.0^\circ \pm 18.1^\circ$  ( $p < 0.01$  for both BI and AAD). The mean coronal joint inclination for controls was  $110.3^\circ \pm 4.23^\circ$ , and in patients with BI and AAD, it

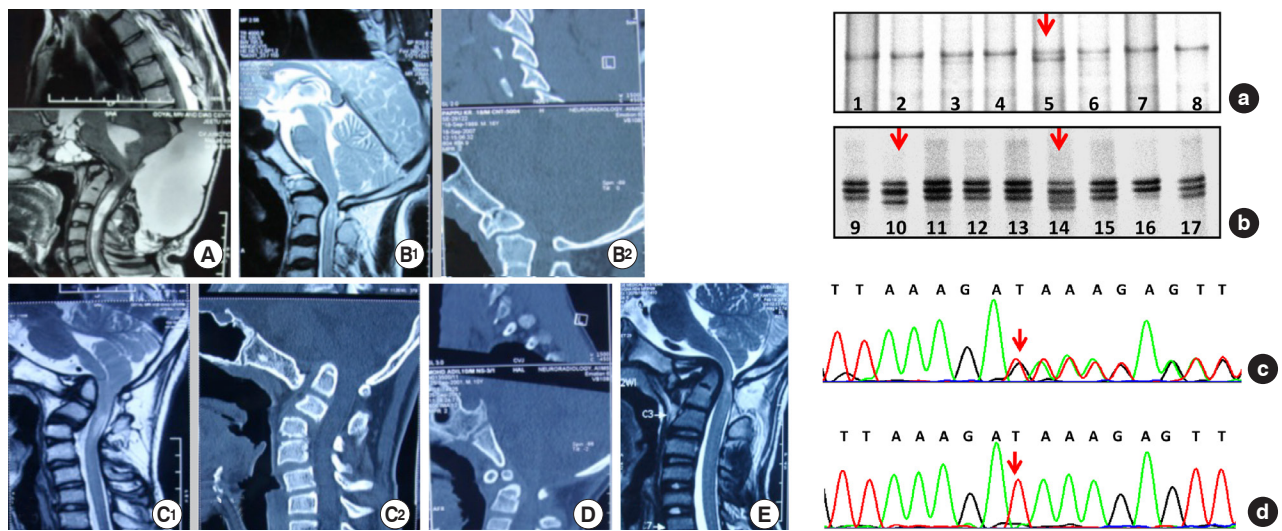


**Fig. 5.** Radiological profiles of patients with change del TCTTTA in exon 25 and 26 in the *FBNI* gene. (A) Magnetic resonance imaging (MRI) investigation showing basilar invagination, atlantoaxial dislocation, clival segmentation, Chiari malformation I and syringomyelia in the patient (B1) and (B2) MRI and computed tomography (CT) scan of the patient showing basilar invagination and clival segmentation, (C1) and (C2) MRI and CT scan of the patient showing basilar invagination and atlantoaxial dislocation, (D) CT scan of the patient showing basilar invagination and atlantoaxial dislocation, (E) MRI of the patient showing Basilar invagination, atlantoaxial dislocation and Chiari malformation type I with a large posterior fossa cyst. Single-stranded conformation polymorphism (SSCP) and sequencing analysis (right panel) of variant IVS25+55-+60delTCTTTA in exon 25 and 26 of the *FBNI* gene. (a, b) SSCP gel picture showing the DNA band shift in lane 5, 10, and 14 (indicated by arrow). (c) Chromatogram showing the heterozygous change (indicated by the red arrow). (d) Chromatogram showing the base sequence of normal control in the same region.

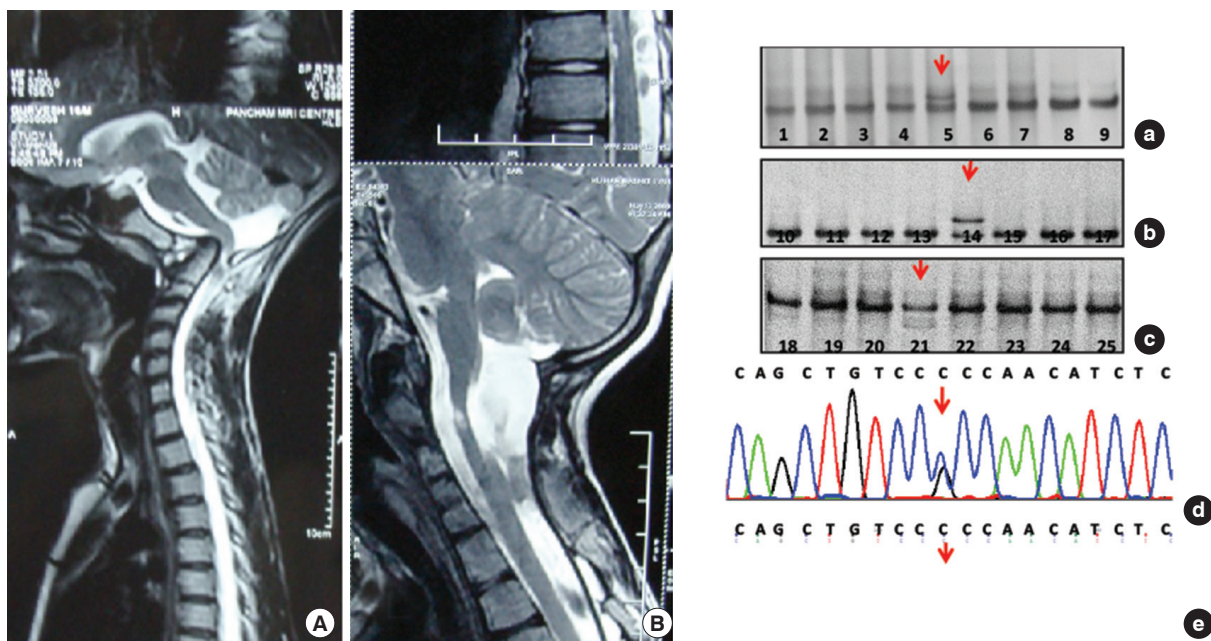


**Fig. 6.** Radiological profile of patients with change P1148A in exon. (A) Magnetic resonance imaging (MRI) of the patient showing basilar invagination, atlantoaxial dislocation, occipitalized C1 arch, and clival segmentation. (B) MRI of the patient showing the basilar invagination and clival segmentation. (Right panel) (a-c) Single-stranded conformation polymorphism gel picture showing the DNA band shift in the lane 5, 14, and 21 (indicated by arrow) in 3 patients in exon 27 of *FBNI* gene. (d) Chromatogram showing heterozygous change (indicated by the red arrow), confirmed as a single base substitution C>G at position c.3441 or P1148A. (e) Chromatogram showing the base sequence of normal control in the same region.



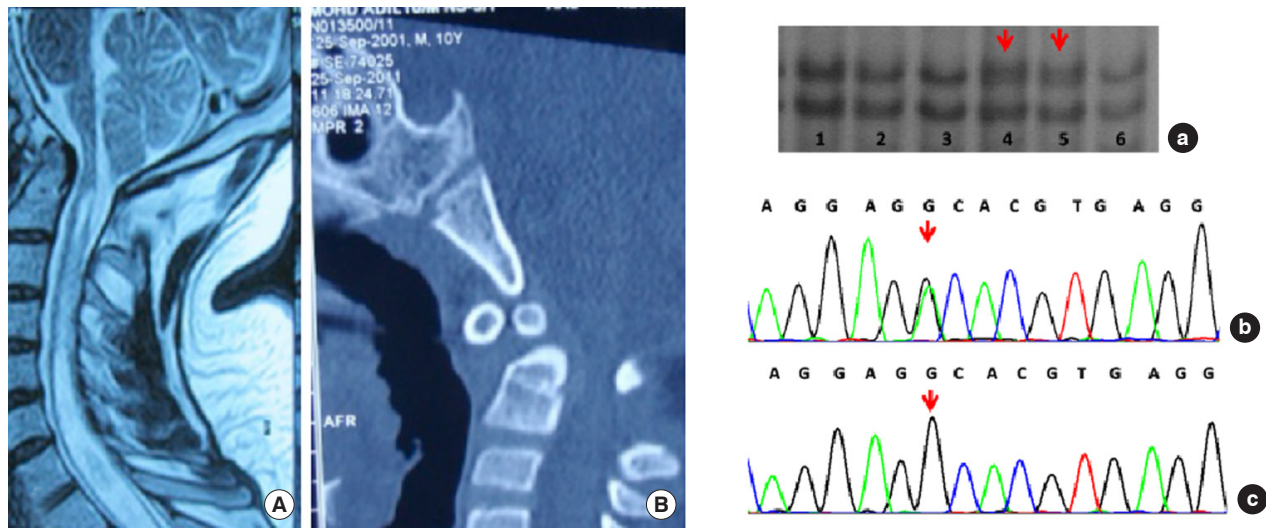


**Fig. 7.** Radiological profiles of patients with change c.1059+12 G>A in exon 3 of PAX1 gene. (A) The patient's magnetic resonance imaging scan shows basilar invagination, Chiari malformation I, and syringomyelia. (B) Computed tomography scan of the patient showing basilar invagination, atlantoaxial dislocation clival segmentation. Single-stranded conformation polymorphism (SSCP) and sequencing analysis of variant c.1059+12 G>A. (Right panel) (a) SSCP gel picture showing the DNA band shifts in lane 4 and 5 (indicated by arrow) in 3 patients. (b) Chromatogram developed by DNA sequencing of these 2 patients showing a single base substitution G>A at position c.1059+12. (c) Chromatogram of the same region of normal control.

was  $125.15^{\circ} \pm 16.4^{\circ}$  (the mean p-value between the right and left joints was 0.2, for BI but not AAD). Finally, joint nonreciprocity also correlated significantly with BI and AAD, i.e., the higher the nonreciprocity, the more severe the BI and AAD.

## DISCUSSION

In the present study, firstly, we have obtained DNA sequence variants in 39 patients (78%). Secondly, we found a new combination of DNA sequence variants, which were reported earlier in isolation as polymorphism. Still, to the best of our knowledge, no earlier study has reported this combination of sequence variants. Third, the study provides a clue that the “non-syndromic” bony CV junction anomalies commonly seen in our set up maybe a “softer variant” of MFS. Despite the less known etiopathology, somatic markers such as the short neck, low hairline, low set ears, and systemic anomalies suggest an underlying genetic basis. However, no constant cluster of phenotypic anomalies or spine structural defects has been reported except BI and AAD, which forms the common denominator.<sup>45</sup> The present study’s findings are important from a treatment point of view as it strengthens the fact that one of the essential components of the pathology is the presence of defective ‘holding’ ligaments that have led to progressive telescoping of the cervical spine into the skull base. This provides a fundamental

basis for treating the pathology by utilizing joint distraction and deformity correction through a posterior approach rather than performing a trans-oral decompression of the odontoid process.<sup>25,46,47</sup> The latter surgical assumption is based on a hypothesis that this deformity is “irreducible,” a fact that is slowly changing to understand that most of these anomalies are reducible.<sup>25,46,47</sup> Our study provides molecular rationale to this changing concept.

Defects in *FBN1* expression results in abnormal elastic fibres, leading to skeletal and cardiovascular anomalies in MFS.<sup>48</sup> The genetic abnormalities in MFS produce a wide range of results, ranging from 10%–100% mutant fibrillin. This results in a substantial phenotypic range of severity.<sup>48</sup> Further, these anomalies are also associated with various other genetic syndromes. Hence, there is a possibility these anomalies of the cervical spine are the variable expression of a connective tissue disorder or a new syndrome in which there is an involvement of connective tissue malformation. Many known genetic disorders that segregate with CM1 affect mesodermally derived cartilage and/or bone.<sup>8,49</sup>

In this study, the sequence variants obtained in exon 25 and 26 were identified as a 6 base pair deletion delTCTTTA. It was reported as polymorphism in patients with MFS37 and found to be clinically insignificant. The reason behind the presence of this change in both exons is the common intronic region shared by these 2 adjacent exons. Further, in exon 27, 3 patients

showed 3 similar kinds of shifts. When sequenced, we obtained a substitution of C>G change (c.3575C>G) in the exonic region leading to a change in the amino acid sequence proline to alanine (P. Pro1148Ala). Pro1148Ala substitution codes for the 13thcbEGF-like domain in the *FBN1* gene. Although Pro1148 is not directly involved in calcium-binding, it is conserved in the mouse and bovine *FBN1* gene. Proline to alanine changes has also been described in other proteins, leading to various consequences ranging from incorrect folding<sup>50</sup> to a native structure virtually identical to the wild type.<sup>51</sup> Presence of such polymorphism leading to laxity of ligaments may have favoured a posterior approach of joint distraction which has emerged over the past decade as a treatment modality.<sup>21,24,25,52</sup> In a study by Schrijver et al.,<sup>53</sup> a homology search for the *FBN1* amino acids was performed and suggested that alanine (in the place of proline) does not change the native domain structure or its function. Since previously, the Pro1148Ala substitution had been identified in individuals affected with MFS, aortic disease, and Shprintzen–Goldberg syndrome and numerous unaffected family members, but only once in 367 unaffected control samples.<sup>54</sup> It was considered to be a potential predisposing allele for aortic aneurysm.<sup>54</sup> Substitution of a different proline by alanine in the first EGF-like clotting factor IX domain has been identified in a patient with mild haemophilia B.<sup>55</sup> To explain this substitution's functional consequences, the authors postulated that altered secondary structure could lead to distortion of cofactor binding sites. In other proteins, proline-alanine interchanges have also been associated with abnormal phenotypes.<sup>56,57</sup> The possibility has to be considered that this substitution may not be wholly neutral but could convey a risk factor in aortic disease. Detailed phenotype-genotype correlations may reveal a modifying influence of the P1148A substitution present in *cis* or *trans*. Interestingly, there was complete concordance between the presence of the P1148A substitution and the less common G/A substitution at the intronic region of exon 28. We also obtained complete concordance of this association in 3 patients. Nevertheless, the association is an attractive hypothesis because the P1148A substitution in exon 27 is less than 300 bp upstream of the intron G/A polymorphism.<sup>58</sup> These 2 sequence variants' concordances suggest that this association may be of ancient origin in human evolution. Schrijver et al.<sup>53</sup> also found that P1148A was associated with G/A polymorphism. They suggested that this concordance may be due to linkage disequilibrium.

The new combination of DNA sequence variants that we have found in our study is 5-base pair deletion delTTTTTA and

a substitution G/A in 11 subjects in exon 28. Both changes were reported in isolation,<sup>58,59</sup> but not in combination. More investigation is needed, but there are equal possibilities that this combination may have some indirect role with the “main etiogenic agent” for CVJ anomalies along with evolutionary linkage disequilibrium.

Most of the DNA sequence variants which we have detected in our study were also obtained by Chowdhury et al.<sup>60</sup> in the patients with tetralogy of Fallot (which shows similar histopathologic changes to bicuspid aortic valvular disease, other fibrillinopathies and *FBN1* implication in MFS) when screened *FBN1* gene (exon 24–28) in Indian patients Exon 25 and 26 showed deletion of TCTTTA. Similarly, in exon 27, they found P1148A substitution in 5 patients. Further, in exon 28, they found 2 types of intronic changes, a 6 base pair deletion (delATTTTT) and a 5-base pair deletion (delTTATG), which we did not obtain. They suggested an increased incidence of “DNA sequence variants” of the *FBN1* gene (exon 24–28) may account for or coexist with the higher incidence of aortic dilation in the patients with tetralogy of Fallot. The third change that we have found in exon 28, was the deletion of 5-base pair (delGTTAT) detected in 5 patients and 2 controls, is reported as polymorphism (rs72132658).

The elucidation of the genetic contribution to the developmental CVJ anomaly will undoubtedly aid in diagnostic evaluation and surgical planning, and it will allow more accurate genetic counselling regarding the risk of recurrence to relatives in the immediate future. Even though we did not find any systemic anomalies in our study, an underlying knowledge that *FBN1* gene anomalies seen in developmental CVJ anomalies could also precipitate cardiac anomalies should prompt the treating physician more rigorously screen these group of patients. Genetic mechanisms of AAD have not previously been shown. Some of the previous case reports of familial Chiari type I malformation suggests genetic causes. It has been reported earlier that estimates of genetic cases vary from 1/18,000 to 1/1,280. It has been shown that in cases twins with CMI and one set of monozygotic (MZ) triplets, higher concordance observed in MZ twins compared to dizygotic twins. In a separate study involving 364 patients, 12% had at least one close relative with CMI and/or syringomyelia. As CMI is associated with a variety of other genetic conditions, that also provides an evidence for a genetic component. A study showed evidence for linkage to regions on Chromosomes 9 and 15, containing the *FBN1* gene, further supports a genetic role in Chiari malformation. In another study, polymorphism has been reported in *MTHFR* gene,

known to have a role in neural tube defects, in patients with AAD. Characterizing the phenotypic presentation and genetic contribution to CMI will not only provide valuable insight into the complex etiology and pathogenesis of the disorder but also aid in associating the risk of symptoms and risk of CMI in relatives of affected patients.

The other component of this study included studying the joint morphology. Our previous studies,<sup>20,22-24,26</sup> and the current study reiterated that in developmental CVJ with AAD and BI is associated with increased obliquity of the joints. The severity is directly proportional to the severity of the AAD and BI. This is especially so for values of craniocervical tilt and SI. Besides, presence of increased “obliquity” of joints (increasing angulation of SI:SI) has been the fundamental basis of developing the modifications of the surgical technique of DCER (distraction, compression, extension, and reduction).<sup>19,21,25,26</sup> The improvements include “joint remodelling” and “extra-articular distraction”. Joint remodelling is performed when the SI is between 90°–110°, and extra-articular distraction is performed when the joints are entirely vertical (SI: 180°). However, it is also to be remembered that the ligaments around the facet joint and those stabilizing the CVJ are quite strong (namely apical, alar, transverse, accessory, and anterior longitudinal ligaments, tectorial, anterior and posterior atlantooccipital membranes). Hence, we hypothesized that only increased obliquity of joints alone might not be responsible for producing AAD and BI. We have also noticed that most patients with developmental CVJ have somatic markers suggestive of an underlying genetic predisposition but do not fit into any specific genetic syndrome (in our cases, clinodactyly, low set ears and increased first interdigital space; Figs. 1, 2). A majority of our patients also have hyperlaxity of joints. Given all the above findings, we decided to study the FB1 gene, which is also affected in MFS. Based on our radiological findings, we propose a new hypothesis for developing AAD and BI in developmental CVJ. We propose that the presence of structural defects in ligaments (due to FB1 gene polymorphisms) and increased obliquity of joints lead to precipitation of AAD and BI. Since most patients develop symptoms by the 1st–2nd decade, we feel that weight-bearing and mechanical stress are further responsible for precipitating instability.

The study has its limitations, like the relatively small sample size. Radiological examination in first degree relatives could not be performed due to either unavailability of the family members or refusal to consent. Another limitation of the study is the variable sensitivity of SSCP.

We also do agree that the exact cause of joint inclination is not known. The actual etio-pathogenesis may be more complex. We wanted to approach the problem in a manner that it could be understood from a clinical perspective. The underlying question was that if the joint morphometry was abnormal, why do most of our patients present between 1st–3rd decade? Effect of gravity obviously plays a role. But the question was again that why do these anomalies present in mostly in younger ages? That is when we thought of exploring the *FBN1* mutations which is responsible for encoding for the formation of ligamentous structures and is abnormal in MFS. Additionally, many of our patients presented with phenotypic features of Marfan's (e.g., hyper-extendibility of fingers etc.). This further prompted us to study this gene. However, further studies will be required in this direction to have more clarity.

## CONCLUSION

A significant number of DNA sequence variants in patients with developmental CVJ anomalies signifies that these variants may not be directly pathogenic, but they are showing association genetically. The DNA sequence variants in these anomalies were also reported in MFS. Our study suggests that the non-syndromic developmental CVJ anomalies so commonly encountered in our clinical situation may be a “subtler version” of MFS or similar connective tissue disorders in which *FBN1* is involved. Furthermore, the presence of abnormalities in joint morphology in the form of increased obliquity may also lead to AAD and BI precipitation. The present study is interesting because it provides further guidance to establish a genetic basis for developmental CVJ anomalies. However, more intensive investigations with some more genes along with *FBN1* are needed in a large cohort of patients. However, a combination of factors like weakened “holding ligaments,” increased obliquity of joints, weight-bearing, etc., may precipitate the AAD and BI in patients with developmental CVJ anomalies.

## CONFLICT OF INTEREST

The authors have nothing to disclose.

## ACKNOWLEDGMENTS

This study was supported by a grant from Department of Biotechnology, Ministry of Science and Technology, India.

## REFERENCES

1. Menezes AH. Craniocervical developmental anatomy and its implications. *Childs Nerv Syst* 2008;24:1109-22.
2. McRAE DL. Bony abnormalities in the region of the foramen magnum: correlation of the anatomic and neurologic findings. *Acta radiol* 1953;40:335-54.
3. Burke SW, French HG, Roberts JM, et al. Chronic atlantoaxial instability in Down syndrome. *J Bone Joint Surg Am* 1985;67:1356-60.
4. Cremers MJ, Bol E, de Roos F, et al. Risk of sports activities in children with Down's syndrome and atlantoaxial instability. *Lancet* 1993;342:511-4.
5. Kopits SE. Orthopedic complications of dwarfism. *Clin Orthop Relat Res* 1976;(114):153-79.
6. Hobbs WR, Sponseller PD, Weiss AP, et al. The cervical spine in Marfan syndrome. *Spine (Phila Pa 1976)* 1997;22:983-9.
7. Herzka A, Sponseller PD, Pyeritz RE. Atlantoaxial rotatory subluxation in patients with Marfan syndrome. A report of three cases. *Spine (Phila Pa 1976)* 2000;25:524-6.
8. Gripp KW, Scott CI Jr, Nicholson L, et al. Chiari malformation and tonsillar ectopia in twin brothers and father with autosomal dominant spondylo-epiphyseal dysplasia tarda. *Skeletal Radiol* 1997;26:131-3.
9. Miller JH, Limbrick DD, Callen M, et al. Spontaneous resolution of Chiari malformation Type I in monozygotic twins. *J Neurosurg Pediatr* 2008;2:317-9.
10. Kirlew KA, Hathout GM, Reiter SD, et al. Os odontoideum in identical twins: perspectives on etiology. *Skeletal Radiol* 1993;22:525-7.
11. Morgan MK, Onofrio BM, Bender CE. Familial os odontoideum. Case report. *J Neurosurg* 1989;70:636-9.
12. Stevens CA, Pearce RG, Burton EM. Familial odontoid hypoplasia. *Am J Med Genet A* 2009;149A:1290-2.
13. Wang S, Wang C. Familial dystopic os odontoideum: a report of three cases. *J Bone Joint Surg Am* 2011;93:e44.
14. Coria F, Quintana F, Rebollo M, et al. Occipital dysplasia and Chiari type I deformity in a family. Clinical and radiological study of three generations. *J Neurol Sci* 1983;62:147-58.
15. Bull JW, Nixon WL, Pratt RT. The radiological criteria and familial occurrence of primary basilar impression. *Brain* 1955;78:229-47.
16. Erickson TC, Paul LW, Suckle HM. Clinical observations on basilar impression of the skull. *Trans Am Neurol Assoc* 1950;51:180-3.
17. Paradis RW, Sax DS. Familial basilar impression. *Neurology* 1972;22:554-60.
18. Joaquim AF, Tedeschi H, Chandra PS. Controversies in the surgical management of congenital craniocervical junction disorders - A critical review. *Neurol India* 2018;66:1003-15.
19. Chandra PS, Singh P. In reply: distraction, compression, extension, and reduction combined with joint remodeling and extra-articular distraction: description of 2 new modifications for its application in basilar invagination and atlantoaxial dislocation: prospective study in 79 cases. *Neurosurgery* 2017;80:231-5.
20. Chandra PS. In reply: different facets in management of congenital atlantoaxial dislocation and basilar invagination. *Neurosurgery* 2015;77:E987-8.
21. Chandra PS, Prabhu M, Goyal N, et al. Distraction, compression, extension, and reduction combined with joint remodeling and extra-articular distraction: description of 2 new modifications for its application in basilar invagination and atlantoaxial dislocation: prospective study in 79 cases. *Neurosurgery* 2015;77:67-80.
22. Chandra PS, Goyal N. In reply: the severity of basilar invagination and atlantoaxial dislocation correlates with sagittal joint inclination, coronal joint inclination, and craniocervical tilt: a description of new indices for the craniovertebral junction. *Neurosurgery* 2015;76:E235-9.
23. Chandra PS. In reply: distraction, compression, and extension reduction of basilar invagination and atlantoaxial dislocation. *Neurosurgery* 2015;76:E240-2.
24. Chandra PS, Goyal N, Chauhan A, et al. The severity of basilar invagination and atlantoaxial dislocation correlates with sagittal joint inclination, coronal joint inclination, and craniocervical tilt: a description of new indexes for the craniovertebral junction. *Neurosurgery* 2014;10 Suppl 4:621-9.
25. Chandra PS, Kumar A, Chauhan A, et al. Distraction, compression, and extension reduction of basilar invagination and atlantoaxial dislocation: a novel pilot technique. *Neurosurgery* 2013;72:1040-53.
26. Sarat Chandra P, Bajaj J, Singh PK, et al. Basilar invagination and atlantoaxial dislocation: reduction, deformity correction and realignment using the DCER (distraction, compression, extension, and reduction) technique with customized instrumentation and implants. *Neurospine* 2019;16:231-50.
27. Bharucha EP, Dastur HM. Craniovertebral anomalies (a report on 40 cases). *Brain* 1964;87:469-80.

28. Boyles AL, Enterline DS, Hammock PH, et al. Phenotypic definition of Chiari type I malformation coupled with high-density SNP genome screen shows significant evidence for linkage to regions on chromosomes 9 and 15. *Am J Med Genet A* 2006;140:2776-85.
29. Urbizu A, Toma C, Poca MA, et al. Chiari malformation type I: a case-control association study of 58 developmental genes. *PLoS One* 2013;8:e57241.
30. Sakai LY, Keene DR, Renard M, et al. FBN1: The disease-causing gene for Marfan syndrome and other genetic disorders. *Gene* 2016;591:279-91.
31. Tiecke F, Katzke S, Booms P, et al. Classic, atypically severe and neonatal Marfan syndrome: twelve mutations and genotype-phenotype correlations in FBN1 exons 24-40. *Eur J Hum Genet* 2001;9:13-21.
32. Schrijver I, Liu W, Brenn T, et al. Cysteine substitutions in epidermal growth factor-like domains of fibrillin-1: distinct effects on biochemical and clinical phenotypes. *Am J Hum Genet* 1999;65:1007-20.
33. Faivre L, Collod-Beroud G, Loeys BL, et al. Effect of mutation type and location on clinical outcome in 1,013 probands with Marfan syndrome or related phenotypes and FBN1 mutations: an international study. *Am J Hum Genet* 2007;81:454-66.
34. Faivre L, Masurel-Paulet A, Collod-Bérout G, et al. Clinical and molecular study of 320 children with Marfan syndrome and related type I fibrillinopathies in a series of 1009 probands with pathogenic FBN1 mutations. *Pediatrics* 2009;123:391-8.
35. Green MR, Sambrook J. *Molecular cloning: laboratory manual*. 4th ed. Cold Spring Harbor (NY): Cold Spring Harbor Laboratory Press; 2012.
36. Miller MS, Cronin MT. Genetic polymorphisms and susceptibility to disease. Chapter PCR: Method and limitations. New York: Taylor and Francis; 2000.
37. Körkkö J, Kaitila I, Lönnqvist L, et al. Sensitivity of conformation sensitive gel electrophoresis in detecting mutations in Marfan syndrome and related conditions. *J Med Genet* 2002;39:34-41.
38. Goel A, Shah A, Gupta SR. Craniovertebral instability due to degenerative osteoarthritis of the atlantoaxial joints: analysis of the management of 108 cases. *J Neurosurg Spine* 2010;12:592-601.
39. Jian FZ, Chen Z, Wrede KH, et al. Direct posterior reduction and fixation for the treatment of basilar invagination with atlantoaxial dislocation. *Neurosurgery* 2010;66:678-87.
40. Smith JS, Shaffrey CI, Abel MF, et al. Basilar invagination. *Neurosurgery* 2010;66(3 Suppl):39-47.
41. Teodori JB, Painter MJ. Basilar impression in children. *Pediatrics* 1984;74:1097-9.
42. Wadia NH. Myelopathy complicating congenital atlanto-axial dislocation. (A study of 28 cases). *Brain* 1967;90:449-72.
43. Wackenheim A. *Roentgen diagnosis of the cranio-vertebral region*. New York: Springer-Verlag; 1974.
44. Mcrae DL, Barnum AS. Occipitalization of the atlas. *Am J Roentgenol Radium Ther Nucl Med* 1953;70:23-46.
45. Yerramneni VK, Chandra PS, Kale SS, et al. A 6-year experience of 100 cases of pediatric bony craniovertebral junction abnormalities: treatment and outcomes. *Pediatr Neurosurg* 2011;47:45-50.
46. Goel A. Treatment of basilar invagination by atlantoaxial joint distraction and direct lateral mass fixation. *J Neurosurg Spine* 2004;1:281-6.
47. Chandra PS. In reply. *Neurosurgery* 2014;74:E148-50.
48. Dietz HC, Pyeritz RE. Mutations in the human gene for fibrillin-1 (FBN1) in the Marfan syndrome and related disorders. *Hum Mol Genet* 1995;4 Spec No:1799-809.
49. Pauli RM, Horton VK, Glinski LP, et al. Prospective assessment of risks for cervicomedullary-junction compression in infants with achondroplasia. *Am J Hum Genet* 1995;56:732-44.
50. Ishihara N, Yamashina S, Sakaguchi M, et al. Malfolded cytochrome P-450(M1) localized in unusual membrane structures of the endoplasmic reticulum in cultured animal cells. *J Biochem* 1995;118:397-404.
51. Dodge RW, Scheraga HA. Folding and unfolding kinetics of the proline-to-alanine mutants of bovine pancreatic ribonuclease A. *Biochemistry* 1996;35:1548-59.
52. Goel A, Sharma P. Craniovertebral realignment for basilar invagination and atlantoaxial dislocation secondary to rheumatoid arthritis. *Neurol India* 2004;52:338-41.
53. Schrijver I, Liu W, Francke U. The pathogenicity of the Pro1148Ala substitution in the FBN1 gene: causing or predisposing to Marfan syndrome and aortic aneurysm, or clinically innocent? *Hum Genet* 1997;99:607-11.
54. Sood S, Eldadah ZA, Krause WL, et al. Mutation in fibrillin-1 and the Marfanoid-craniosynostosis (Shprintzen-Goldberg) syndrome. *Nat Genet* 1996;12:209-11.
55. Spitzer SG, Kuppaswamy MN, Saini R, et al. Factor IXHollywood: substitution of Pro55 by Ala in the first epidermal growth factor-like domain. *Blood* 1990;76:1530-7.
56. Ivanoff LA, Looney DJ, McDanal C, et al. Alteration of HIV-

- 1 infectivity and neutralization by a single amino acid replacement in the V3 loop domain. *AIDS Res Hum Retroviruses* 1991;7:595-603.
57. Janssen OE, Takeda K, Refetoff S. Sequence of the variant thyroxine-binding globulin (TBG) in a Montreal family with partial TBG deficiency. *Hum Genet* 1991;87:119-22.
58. Tynan K, Comeau K, Pearson M, et al. Mutation screening of complete fibrillin-1 coding sequence: report of five new mutations, including two in 8-cysteine domains. *Hum Mol Genet* 1993;2:1813-21.
59. Nijbroek G, Sood S, McIntosh I, et al. Fifteen novel FBN1 mutations causing Marfan syndrome detected by heteroduplex analysis of genomic amplicons. *Am J Hum Genet* 1995; 57:8-21.
60. Chowdhury UK, Mishra AK, Balakrishnan P, et al. Role of fibrillin-1 genetic mutations and polymorphism in aortic dilatation in patients undergoing intracardiac repair of tetralogy of Fallot. *J Thorac Cardiovasc Surg* 2008;136:757-66, 766.e1-10.